ORAI1 and ORAI2 modulate murine neutrophil calcium signaling, cellular activation, and host defense

Derayvia Grimes[a,1], Ryan Johnson[a,1], Madeline Pashos[a], Celeste Cummings[a], Chen Kang[b], Georgia R. Sampedro[a], Eric Tycksen[c], Helen J. McBride[d], Rajan Sah[b], Clifford A. Lowell[e], and Regina A. Clemens[a,2]

[a]Department of Pediatrics, Washington University School of Medicine, St. Louis, MO 63110; [b]Department of Internal Medicine, Washington University School of Medicine, St. Louis, MO 63110; [c]McDonnell Genome Institute, Washington University School of Medicine, St. Louis, MO 63110; [d]Inflammation Research, Amgen, Thousand Oaks, CA 91320; and [e]Department of Laboratory Medicine, University of California, San Francisco, CA 94143

Edited by Michael D. Cahalan, University of California, Irvine, CA, and approved August 11, 2020 (received for review May 5, 2020)

Calcium signals are initiated in immune cells by the process of store-operated calcium entry (SOCE), where receptor activation triggers transient calcium release from the endoplasmic reticulum, followed by opening of plasma-membrane calcium-release activated calcium (CRAC) channels. ORAI1, ORAI2, and ORAI3 are known to comprise the CRAC channel; however, the contributions of individual isoforms to neutrophil function are not well understood. Here, we show that loss of ORAI1 partially decreases calcium influx, while loss of both ORAI1 and ORAI2 completely abolishes SOCE. In other immune-cell types, loss of ORAI2 enhances SOCE. In contrast, we find that ORAI2-deficient neutrophils display decreased calcium influx, which is correlated with measurable differences in the regulation of neutrophil membrane potential via KCa3.1. Decreased SOCE in ORAI1-, ORAI2-, and ORAI1/2-deficient neutrophils impairs multiple neutrophil functions, including phagocytosis, degranulation, leukotriene, and reactive oxygen species (ROS) production, rendering ORAI1/2-deficient mice highly susceptible to staphylococcal infection. This study demonstrates that ORAI1 and ORAI2 are the primary components of the neutrophil CRAC channel and identifies subpopulations of neutrophils where cell-membrane potential functions as a rheostat to modulate the SOCE response. These findings have implications for mechanisms that modulate neutrophil function during infection, acute and chronic inflammatory conditions, and cancer.

neutrophil | membrane potential | calcium signaling | store-operated calcium entry | ORAI1

Neutrophils are increasingly appreciated to display a diverse array of phenotypes and behaviors; however, the signaling pathways that govern neutrophil responses are incompletely understood. As a central signaling mediator, cytoplasmic calcium concentrations are tightly controlled, and, in resting cells, calcium is sequestered outside the cell or within organelles such as the endoplasmic reticulum (ER). Calcium entry into neutrophils occurs primarily by store-operated calcium entry (SOCE), whereby receptor activation initiates a signaling cascade, culminating in activation of phospholipases, which liberate diacylglycerol and inositol triphosphate (IP_3) from membrane-bound phosphatidylinositol 4,5-bisphosphate (1). IP_3 binding to the ER IP_3 receptor releases "store" calcium from the ER, resulting in transient elevation of cytoplasmic calcium. Stromal interaction molecule (STIM) calcium sensors in the ER membrane undergo oligomerization and conformational change triggered by ER calcium depletion and gate calcium-release activated calcium (CRAC) channels in the plasma membrane. Opening of these channels allows sustained calcium entry into the cell and activation of calcium-dependent cellular processes.

The CRAC channel is a hexamer comprising varying ratios of three ORAI family members, ORAI1, ORAI2, and ORAI3. When overexpressed with STIM1, all three isoforms display features characteristic of CRAC channels, signified by an inwardly rectifying, highly calcium-selective, low-conductance current and fast calcium-dependent inactivation (2, 3). Expression patterns and differences in isoform features, such as activation or inactivation kinetics and sensitivity to modulatory factors, also influence CRAC-channel function (2–10). ORAI1 and ORAI2 are broadly expressed in immune cells, and humans with ORAI1 mutations develop a severe combined immunodeficiency-like immunodeficiency, highlighting the importance of this isoform in immune function (11, 12). In mice, ORAI1 also appears to be the dominant functional isoform in immune cells, with substantial deficits in ORAI1-deficient T cells, mast cells, and platelet SOCE (11, 13, 14). The role of ORAI2 is less clear; however, a recent report by Vaeth et al. (15) demonstrated that in naïve CD4+ T cells, dendritic cells, and macrophages, ORAI2 appears to play a modulatory role, such that deletion of ORAI2 enhances SOCE. Mice with deletion of ORAI2 combined with T cell-specific deletion of ORAI1 are protected in models of graft vs. host disease, but are more susceptible to viral infection, demonstrating the relevance of this signaling pathway in T cell-mediated immune responses (15).

Calcium influx mediates critical neutrophil functions, such as phagocytosis, degranulation, reactive oxygen species (ROS) production, and cytokine synthesis (16–26), but less is known about the molecular machinery that drives SOCE in neutrophils. Previous work from our group and others demonstrated that

Significance

Neutrophils are essential for host defense against pathogens. Although calcium signals direct numerous cell functions, the molecular machinery that orchestrates calcium influx into neutrophils is poorly defined. We demonstrate that ORAI1 and ORAI2 are key components of the mouse neutrophil calcium release-activated calcium channel and are essential for neutrophil bactericidal function. We find that neutrophils separate into two populations with distinct regulation of the membrane potential during calcium influx, which influences the magnitude of SOCE and the effect of ORAI isoform deficiency. These findings advance understanding of the mechanics of neutrophil calcium signaling, identify neutrophil subpopulations where the cell-membrane potential modulates the calcium response, and suggest mechanisms that regulate neutrophil function during infection and inflammation.

Author contributions: C.K., G.R.S., R.S., C.A.L., and R.A.C. designed research; D.G., R.J., M.P., C.C., C.K., G.R.S., and R.A.C. performed research; E.T., H.J.M., and R.S. contributed new reagents/analytic tools; C.K., E.T., and R.A.C. analyzed data; and R.A.C. wrote the paper.

Competing interest statement: H.J.M. was an employee and shareholder of Amgen, Inc. at the time the studies were performed.

This article is a PNAS Direct Submission.

[1]D.G. and R.J. contributed equally to this work.

[2]To whom correspondence may be addressed. Email: clemensra@wustl.edu.

This article contains supporting information online at https://www.pnas.org/lookup/suppl/doi:10.1073/pnas.2008032117/-/DCSupplemental.

First published September 14, 2020.

STIM1 and STIM2 cooperatively regulate neutrophil SOCE; however, the role of different ORAI channel components is less clear (19, 27). While knockdown of ORAI1 in neutrophil-like cell lines impairs SOCE, results from primary human and mouse neutrophils have been mixed, with either moderately decreased or normal SOCE observed in ORAI1-deficient neutrophils (24, 28–32). The reason for these discrepancies is unclear; however, across all studies, loss of ORAI1 at most only partially impairs SOCE, implying that other channel components, such as ORAI2 or ORAI3, also contribute to SOCE in neutrophils.

Here, we show that ORAI1 and ORAI2 are the predominant ORAI isoforms expressed in mouse neutrophils and that their expression is differentially regulated by inflammatory stimuli. Using mice with hematopoietic deletion of *Orai1* and/or *Orai2*, we show that SOCE is diminished in the absence of ORAI1 and completely abolished in double-mutant cells. In contrast to other immune-cell types, deletion of *Orai2* impairs, rather than augments, SOCE in mouse neutrophils. In investigating the mechanism underlying this neutrophil-specific phenotype, we observed that bone marrow neutrophils display heterogeneous calcium responses due to differential regulation of their membrane potential. Decreased expression of the calcium-activated potassium channel, KCa3.1, results in depolarization in a subset of neutrophils and correlates with impaired SOCE in ORAI2 mutant neutrophils. Collectively, these results demonstrate that ORAI1 and ORAI2 are the primary components of the neutrophil CRAC channel and cooperatively regulate calcium-dependent neutrophil responses and host defense against *Staphylococcus aureus*. Furthermore, this study highlights cell-membrane potential as a critical modulator of SOCE in neutrophil subsets. This discovery has the potential to lead to targets for modulating neutrophil activity in infection or inflammatory conditions such as in cystic fibrosis, gout, and cancer.

Results

Orai1 and _Orai2_ Are the Predominant CRAC-Channel Isoforms Expressed in Neutrophils and Are Differentially Expressed in Neutrophils Based on Location and Inflammatory Context. Calcium signals initiated by SOCE are critical for an array of neutrophil functions; however, while the calcium sensors STIM1 and STIM2 have been recently studied (26, 27, 33), the composition and contribution of individual CRAC-channel components are not well defined. To explore which channel components support neutrophil SOCE, we performed qRT-PCR on neutrophils sorted from mouse bone marrow, blood, and spleen (Fig. 1 *A* and *B*). There were slight differences in ORAI expression at different sites; however, *Orai1* was the predominant isoform in neutrophils, with expression ~5-fold higher than *Orai2* and ~12-fold higher than *Orai3*. In comparison, naïve CD4+ T cells had lower expression of all isoforms, particularly *Orai1* and *Orai3*. Of note, the Immgen microarray database (www.immgen.org/databrowser/index.html) reports a predominance of *Orai2* in resting neutrophils; however, this discrepancy is likely the result of signal from the *Orai2* pseudogene, which is nearly identical to the *Orai2* messenger RNA (mRNA) (5). While TRP channels have been proposed to associate with CRAC channels (1, 28, 34), we found low TRP family expression in mouse neutrophils (*SI Appendix*, Fig. S2*A*). ORAI isoform ratios changed after exposure to inflammatory agonists, with the *Orai1:Orai2* expression ratio ranging from 1:1 to 30:1 (predominantly driven by change in *Orai1* expression), depending on the stimulus (Fig. 1*C*), suggesting that modulation of CRAC-channel composition may be important for regulation of neutrophil SOCE during host responses to infection and inflammatory stimuli.

To further probe how CRAC-channel composition contributes to neutrophil SOCE, we generated mice with hematopoietic deletion of ORAI1 and/or ORAI2 by using *Vav–Cre*-mediated deletion of floxed alleles, referred to as $Orai1^{VavCre}$, $Orai2^{VavCre}$, and $Orai1/2^{VavCre}$ (*SI Appendix*, Fig. S1). These mice displayed 100% deletion of *Orai1* and *Orai2* in bone marrow neutrophils (as measured by qPCR) and no significant compensatory alteration in expression of other ORAI isoforms (Fig. 1*D*). ORAI protein largely recapitulated mRNA levels; however, ORAI2 protein was decreased in ORAI1-deficient neutrophils, whole splenocytes, and naïve CD4+ T cells, suggesting that ORAI2 stability is potentially altered in the absence of ORAI1 (Fig. 1 *E* and *F* and *SI Appendix*, Fig. S2 *B* and *C*). $Orai1^{VavCre}$, $Orai2^{VavCre}$, and young $Orai1/2^{VavCre}$ mice had normal numbers of circulating neutrophils with no changes in surface phenotype (*SI Appendix*, Fig. S2 *D–F*). $Orai1/2^{VavCre}$ mice are known to have decreased regulatory T cells and develop lymphoproliferation with age (15). We found that circulating neutrophil numbers were increased in mice >10 wk old; therefore, we used 6-wk-old mice, which had no appreciable difference in resting neutrophil number or surface phenotype (*SI Appendix*, Fig. S2 *D–F*).

ORAI1 and ORAI2 Cooperatively Regulate SOCE in Neutrophils. To analyze the contribution of ORAI1 and ORAI2 to neutrophil SOCE, we measured calcium influx in $Orai1^{VavCre}$, $Orai2^{VavCre}$, and $Orai1/2^{VavCre}$ neutrophils. ER store release induced by the sarcoplasmic–ER calcium ATPase-inhibitor thapsigargin was not altered in ORAI1- and/or ORAI2-deficient cells (Fig. 2*C*). Loss of ORAI1 impaired SOCE, while the absence of both ORAI1 and ORAI2 completely abolished SOCE in neutrophils, suggesting that these proteins are essential for neutrophil CRAC-channel function (Fig. 2 *A* and *B*). Studies in lymphocytes, macrophages, and mast cells have demonstrated enhanced SOCE in ORAI2-deficient cells (15, 35). In contrast, we observed that deletion of *Orai2* in neutrophils impaired SOCE (Fig. 2 *A* and *B* and *SI Appendix*, Fig. S3 *A* and *B*). ORAI2-deficient cells displayed marked sensitivity to extracellular calcium concentration, where higher concentrations of extracellular calcium rescued the defect in ORAI2-deficient, but not ORAI1-deficient, cells (Fig. 2 *D* and *E* and *SI Appendix*, Fig. S3 *C* and *D*). Receptor-dependent activation of SOCE via the G-protein-coupled Formyl Peptide Receptor 1 was decreased in ORAI single- and double-mutant neutrophils, similar to that observed with thapsigargin and ionomycin (*SI Appendix*, Fig. S4 *A* and *B*). Since neutrophil priming with granulocyte–macrophage colony-stimulating factor (GM-CSF) increased the ratio of *Orai1:Orai2* expression (Fig. 1*C*), we evaluated if this would alter the impact of ORAI1 deficiency. Indeed, loss of ORAI1, but not ORAI2, resulted in a more pronounced decrease in SOCE in primed compared to naïve neutrophils (*SI Appendix*, Fig. S4 *C–E*).

Heterogeneous SOCE in Bone Marrow Neutrophils Is Differentially Affected by Loss of ORAI2. To explore why loss of ORAI2 has a different effect in neutrophils compared with other immune cells, we first analyzed features of wild-type (WT) SOCE. Calcium measurements by fluorimetry and kinetic averages of flow-cytometric measurements assume a homogeneous cell population. However, on closer inspection of dot plots, we observed that bone marrow neutrophils segregated into populations with distinct calcium responses. In WT neutrophils, two populations were most apparent at low concentrations (0.5 mM) of extracellular calcium, whereas in higher concentrations of calcium, the populations were visible early in SOCE, but then converged (Fig. 3*A* and *SI Appendix*, Fig. S4*F*). Notably, loss of ORAI1 blunted SOCE in both populations, whereas ORAI2 deficiency predominantly affected SOCE in the lower-calcium (Ca^{lo}) population (Fig. 3 *B–F* and *SI Appendix*, Fig. S4*F*). Together, these data indicate that bone marrow neutrophils are a heterogenous population of cells characterized by distinct SOCE responses and differential impact of ORAI1 and ORAI2 deficiency.

Dichotomous Regulation of Membrane Potential Determines Magnitude of SOCE Response in Neutrophil Subsets. We next explored the mechanism driving this heterogeneous SOCE response. Ion flux across cell membranes is primarily determined by three biochemical

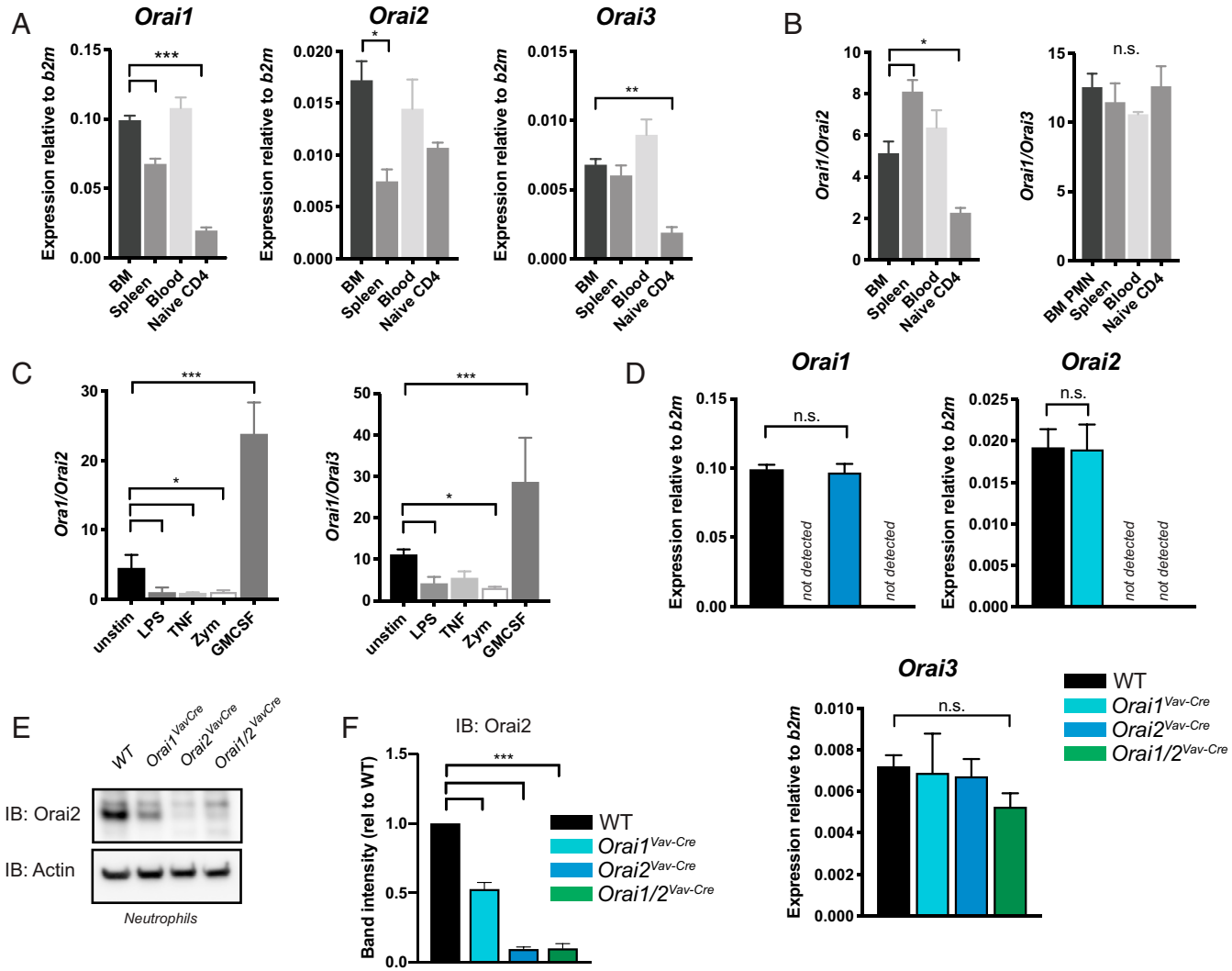

Fig. 1. Expression of Orai channel proteins in neutrophils. (*A* and *B*) Expression levels relative to the reference gene beta-2 microglobulin (*b2m*) (*A*) and isoform ratios (*B*) of *Orai1*, *Orai2*, and *Orai3* in sorted neutrophils from bone marrow (BM), spleen, and blood determined by qRT-PCR. Expression levels in isolated naïve CD4+ T cells are shown for comparison. (*C*) Orai expression ratios in neutrophils stimulated with LPS (1 μg/mL), TNFα (100 ng/mL), zymosan (20 μg/mL), or GM-CSF (100 ng/mL) for 4 h. (*D*) Expression levels of *Orai1*, *Orai2*, and *Orai3* in isolated bone marrow neutrophils from WT, $Orai1^{VavCre}$, $Orai2^{VavCre}$, or $Orai1/2^{VavCre}$ mice. $n = 3$ to 8 independent experiments. (*E*) Western blot analysis of ORAI2 protein levels from neutrophils isolated from WT, $Orai1^{VavCre}$, $Orai2^{VavCre}$, or $Orai1/2^{VavCre}$ mice. (*F*) Quantitation of *E* including data from three independent experiments. One-way ANOVA with Dunnett's adjustment for multiple comparisons (*A*–*D*). One sample *t* test (*F*). $^{*}P < 0.05$; $^{**}P < 0.005$; $^{***}P < 0.0001$. n.s., not significant; rel, relative; unstim, unstimulated; PMN, neutrophil.

properties: 1) chemical gradient (extracellular vs. intracellular ion concentration), 2) transmembrane electrical field (membrane potential/*Vm*), and 3) membrane permeability (channel number and conductance). Since the extracellular calcium concentration is determined by experimental conditions, we postulated that the difference in Ca^{hi} vs. Ca^{lo} populations is driven by changes in membrane potential or channel composition. Intriguingly, neutrophils labeled with the membrane potential indicator DIBAC4(3) and stimulated with ionomycin segregated into two distinct populations; ~40% of cells depolarized (fluorescein isothiocyanate [FITC]-brighter, MP^{depol}), while the rest remained polarized (FITC-lower, MP^{pol}) (Fig. 4 *A* and *C*). The two distinct responses were validated with multiple other membrane-potential indicators and by directly measuring membrane potential through perforated-patch current-clamp measurements (*SI Appendix*, Fig. S5 *A*–*G* and Fig. 4 *D*–*F*).

Influx of positively charged calcium ions will cause cell depolarization (if uncompensated); however, calcium- or voltage-dependent gating of other channels during SOCE can modulate the membrane potential to either enhance or inhibit calcium entry (36). Thus, calcium influx could drive depolarization, or, alternatively, activation of hyperpolarizing currents could drive enhanced SOCE. Intriguingly, co-labeling with calcium and membrane potential indicators revealed that the depolarized neutrophils corresponded to Ca^{lo} cells (Fig. 4*B*). Conversely, neutrophils that remained hyperpolarized had enhanced calcium influx (Fig. 4*B*). These findings indicate that the absolute membrane potential and associated electrochemical driving force during SOCE determines the magnitude of calcium influx in these neutrophil subsets (Fig. 4*G*).

Neutrophils are notoriously sensitive to activation during isolation and manipulation; however, neither population showed surface-marker evidence of activation (CD11b up-regulation or CD62L shedding), and both populations had equivalent levels of the neutrophil marker Ly6G (*SI Appendix*, Fig. S5 *H* and *I*). To determine whether these populations are transcriptionally distinct neutrophil subsets, we performed RNA sequencing (RNAseq) on

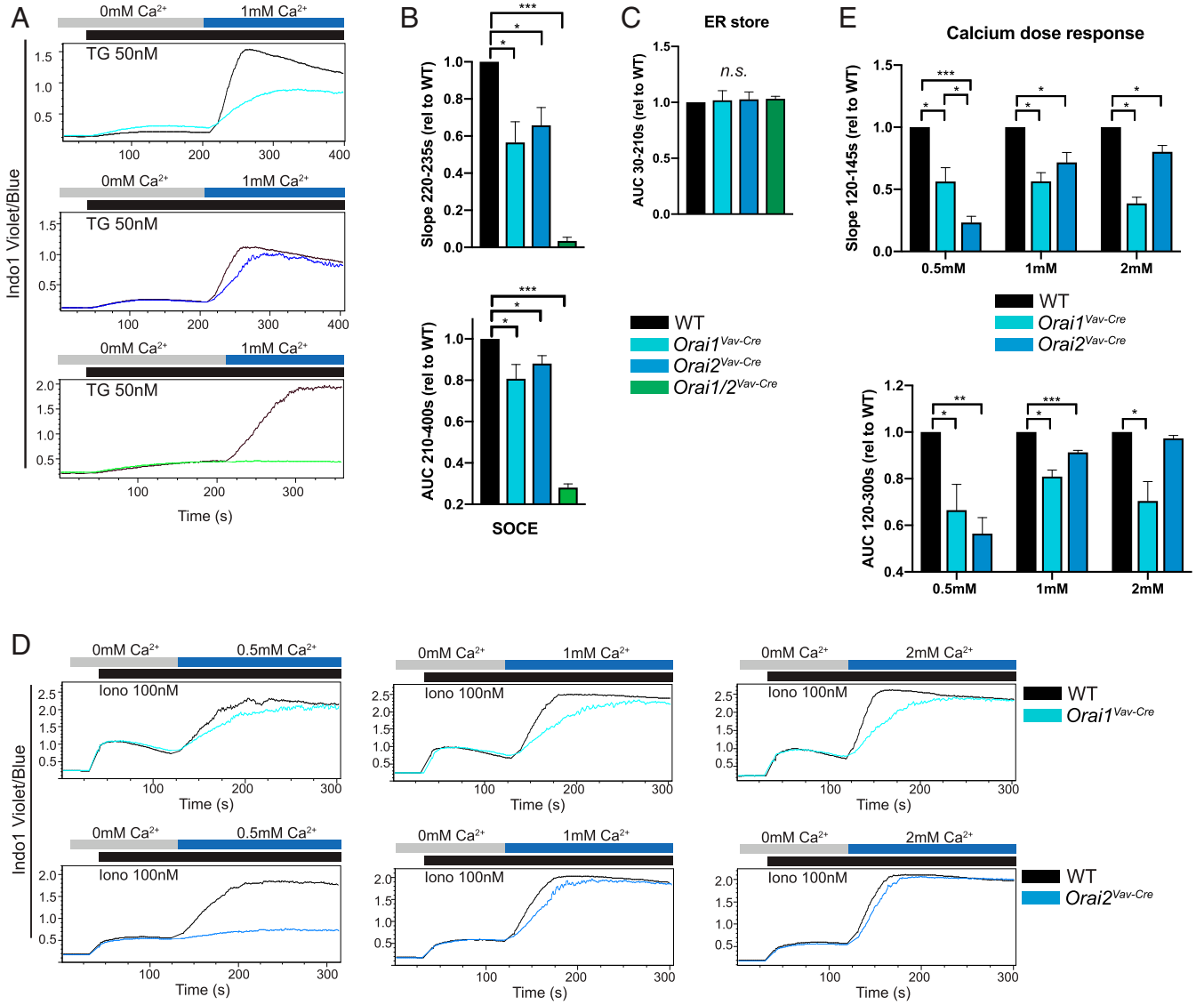

Fig. 2. SOCE in Orai1 and Orai2-deficient neutrophils. (*A*) Calcium influx in bone marrow neutrophils from WT, *Orai1*^{VavCre}, *Orai2*^{VavCre}, or *Orai1/2*^{VavCre} mice, measured by flow cytometry after ER store depletion with thapsigargin (TG; 50 nM) and readdition of 1 mM calcium. (*B*) Quantitation of rate of calcium influx ($Slope_{220–235s}$) (*Upper*) and net calcium influx ($AUC_{210–400s}$), (*Lower*). (*C*) Quantitation of ER store calcium release ($AUC_{30–210s}$). (*D* and *E*) Calcium influx in bone marrow neutrophils from WT, *Orai1*^{VavCre} (*Upper*), or *Orai2*^{VavCre} (*Lower*) mice measured by flow cytometry after ER store depletion with ionomycin (Iono) followed by addition of the indicated calcium concentration. (*E*) Quantitation of *D*. Data shown are representative fluorescence-activated cell sorting (FACS) plots or compiled data from 3 to 10 independent experiments, normalized to WT response. One sample *t* test was used. **P* < 0.05; ***P* < 0.005; ****P* < 0.0001. n.s., not significant. *n* = 3 to 7 independent experiments. AUC, area under the curve; rel, relative.

neutrophils sorted from *Vm* populations, revealing differential expression of ~700 genes, and, in particular, marked down-regulation of primary granule proteins in the MP^{depol} subset (37) (Fig. 4*H* and *SI Appendix*, Fig. S6 *A–C*). Gene Ontology pathway analysis demonstrated decreased growth- and division-related genes, but increased expression of cytokine response and ribosomal/translational machinery in the depolarized subset (*SI Appendix*, Fig. S6*D*). Notably, the RNAseq dataset and confirmatory qPCR demonstrated equivalent expression of ORAI proteins in the subsets (*SI Appendix*, Fig. S6 *E–G*), suggesting that differences in SOCE components do not contribute to the distinct calcium signatures of these two populations.

Phenotype of ORAI2-Deficient Cells Correlates with the State of the Membrane Potential. Since loss of ORAI2 decreased SOCE primarily in depolarized/Ca^{lo} neutrophils, despite equivalent expression levels, we hypothesized that the phenotype of ORAI2-deficient cells might be influenced by the cell-membrane potential. To test this, we pretreated neutrophils with the ionophore gramicidin, which depolarizes cells by increasing permeability to monovalent cations (*SI Appendix*, Fig. S5*C*). As expected, depolarization inhibited SOCE in WT cells. The deficit in ORAI single-mutant neutrophils, however, was exaggerated compared to untreated cells (Fig. 5 *A–E*). Neutrophils are unique in that they produce generous quantities of ROS via the NADPH oxidase. The NADPH oxidase transfers negative charge across the plasma membrane, effectively depolarizing the cell; thus, SOCE under depolarized conditions is particularly relevant for neutrophil function (38, 39). Indeed, phorbol 12-myristate 13-acetate (PMA) pretreatment to induce ROS production depolarized the neutrophils (*SI Appendix*, Fig. S5 *C* and *D*) and augmented the SOCE defect in ORAI single-mutant neutrophils, similar to treatment with gramicidin (*SI Appendix*, Fig. S7 *A–C*).

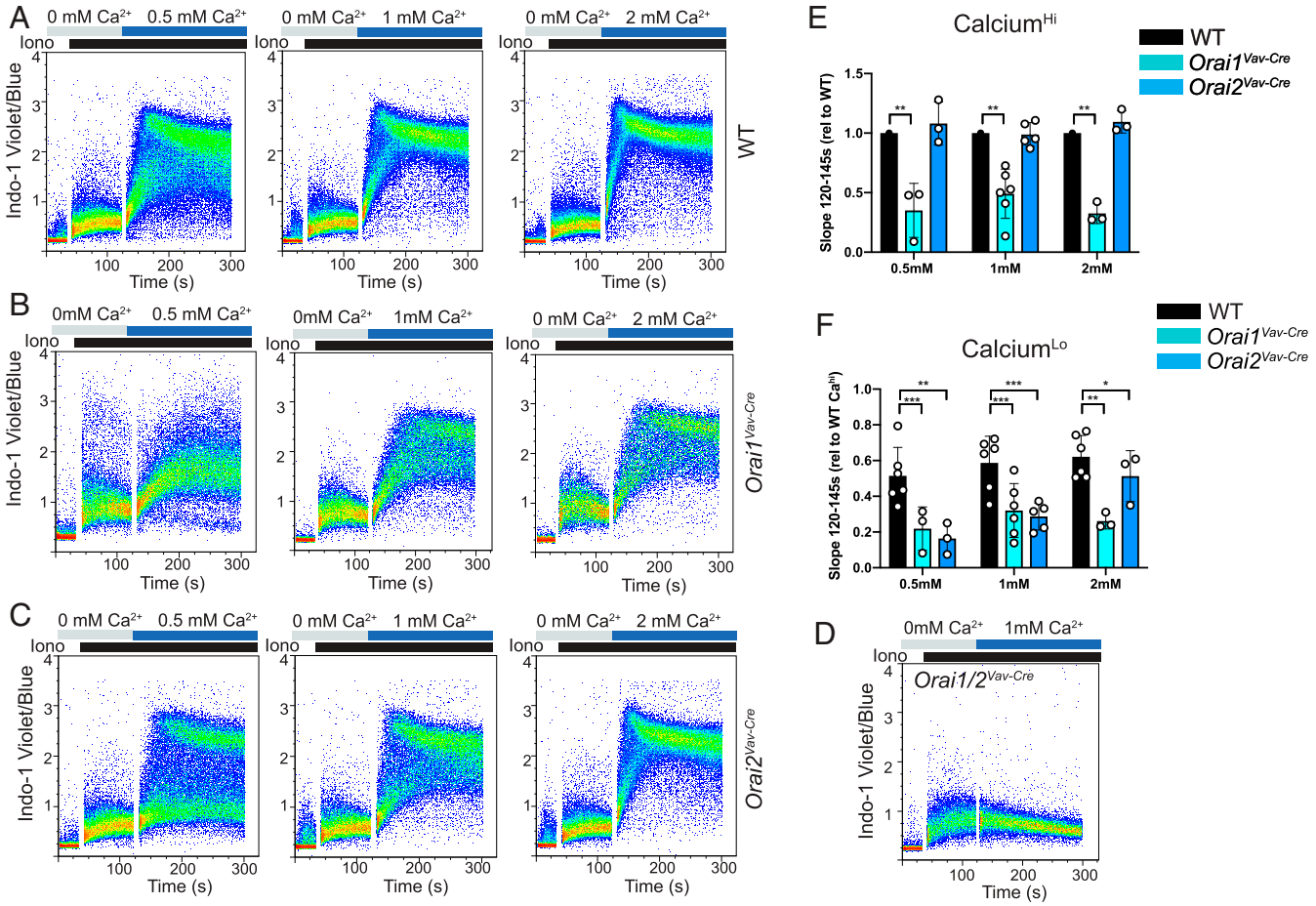

Fig. 3. Heterogeneous response of bone marrow neutrophils to calcium stimuli. (*A–D*) Dot plots of calcium influx in bone marrow neutrophils from WT (*A*), *Orai1*^{VavCre} (*B*), *Orai2*^{VavCre} (*C*), or *Orai1/2*^{VavCre} (*D*) mice, measured by flow cytometry after ER store depletion with 100 nM ionomycin, followed by addition of 0.5, 1, or 2 mM calcium, as indicated. (*E* and *F*) Quantification of SOCE (Slope$_{120–145s}$) in the Ca^{hi} vs. Ca^{lo} neutrophil subsets. Gating approach is shown in *SI Appendix*, Fig. S4*F*. Data shown are representative FACS plots or compiled data from three to six independent experiments, normalized to WT response. Unpaired *t* test. **P* < 0.05; ***P* < 0.005; ****P* < 0.0001. rel, relative.

Since impaired SOCE in ORAI2-deficient neutrophils was evident only in the depolarized population and was augmented when all cells were depolarized with gramicidin or PMA, we next asked whether cell-type-specific regulation of membrane potential could contribute to the opposing SOCE phenotype of ORAI2-deficient neutrophils compared with naïve CD4+ T cells (15). We found that lymphocytes remained polarized throughout stimulation, corresponding to a uniform calcium response (Fig. 5 *F–H*). Similar to Vaeth et al. (15), we observed that SOCE was modestly enhanced in ORAI2-deficient naïve CD4+ T cells (Fig. 5*I*). However, under depolarized conditions (+gramicidin), the phenotype reversed, with ORAI2-deficient naïve CD4+ T cells displaying decreased SOCE compared to WT cells (Fig. 5 *I* and *J* and *SI Appendix*, Fig. S7 *D* and *E*).

Neutrophil Subsets Are Characterized by Differential Expression of Calcium-Activated Potassium Channel KCa3.1/*Kcnn4*. We surmised that the two populations likely have differential expression of a channel that is activated during SOCE and influences the membrane potential. In our RNAseq dataset, components of the mitochondrial calcium uniporter (MCU and MICU2) were slightly more highly expressed in the polarized population; however, treatment with an MCU inhibitor did not change the fraction of cells in each population (*SI Appendix*, Fig. S8 *A–C*). We found no significant differences in K$^+$ channel expression (*SI Appendix*, Fig. S8*D*); however, since voltage- and calcium-gated potassium channels are responsible for the hyperpolarization during SOCE in lymphocytes (40, 41), we tested inhibitors of several candidate potassium channels. While voltage-gated K$^+$ inhibitors Agitoxin (pan-Kv) and Shk1-dap22 (Kv1.3-specific) had no effect on the *Vm* populations (*SI Appendix*, Fig. S8 *E* and *F*), TRAM-34 (KCa3.1 inhibitor) abolished the polarized neutrophil population during SOCE and, therefore, inhibited calcium influx (Fig. 6 *A* and *B*). This channel was not detected by RNAseq; however, dedicated qPCR for *Kcnn4* demonstrated increased expression in the polarized population (Fig. 6*C*). Depolarization of >80% of neutrophils and loss of the Ca^{hi} population with genetic deletion of *Kcnn4* confirmed that KCa3.1 is the primary channel responsible for hyperpolarization and enhanced SOCE in this neutrophil subset (Fig. 6 *D* and *E* and *SI Appendix*, Fig. S8*G*). Finally, since loss of ORAI2 impairs SOCE primarily in the depolarized/Ca^{lo} (KCa3.1-low) subset, we asked whether inhibiting KCa3.1 would further impair SOCE in ORAI2-deficient neutrophils. Indeed, loss of the Ca^{hi} subset with TRAM-34 treatment had a disproportionate effect in ORAI2-deficient neutrophils (Fig. 6 *F* and *G* and *SI Appendix*, Fig. S8*H*).

ORAI1 and ORAI2 Are Required for Neutrophil ROS, Phagocytosis, and LTB4 Production. Calcium is required for numerous neutrophil processes, including activation of the NADPH oxidase, degranulation, and phagocytosis; therefore, we analyzed these neutrophil responses in ORAI1- and/or ORAI2-deficient cells. ROS production induced via several receptors, including the G-protein-coupled

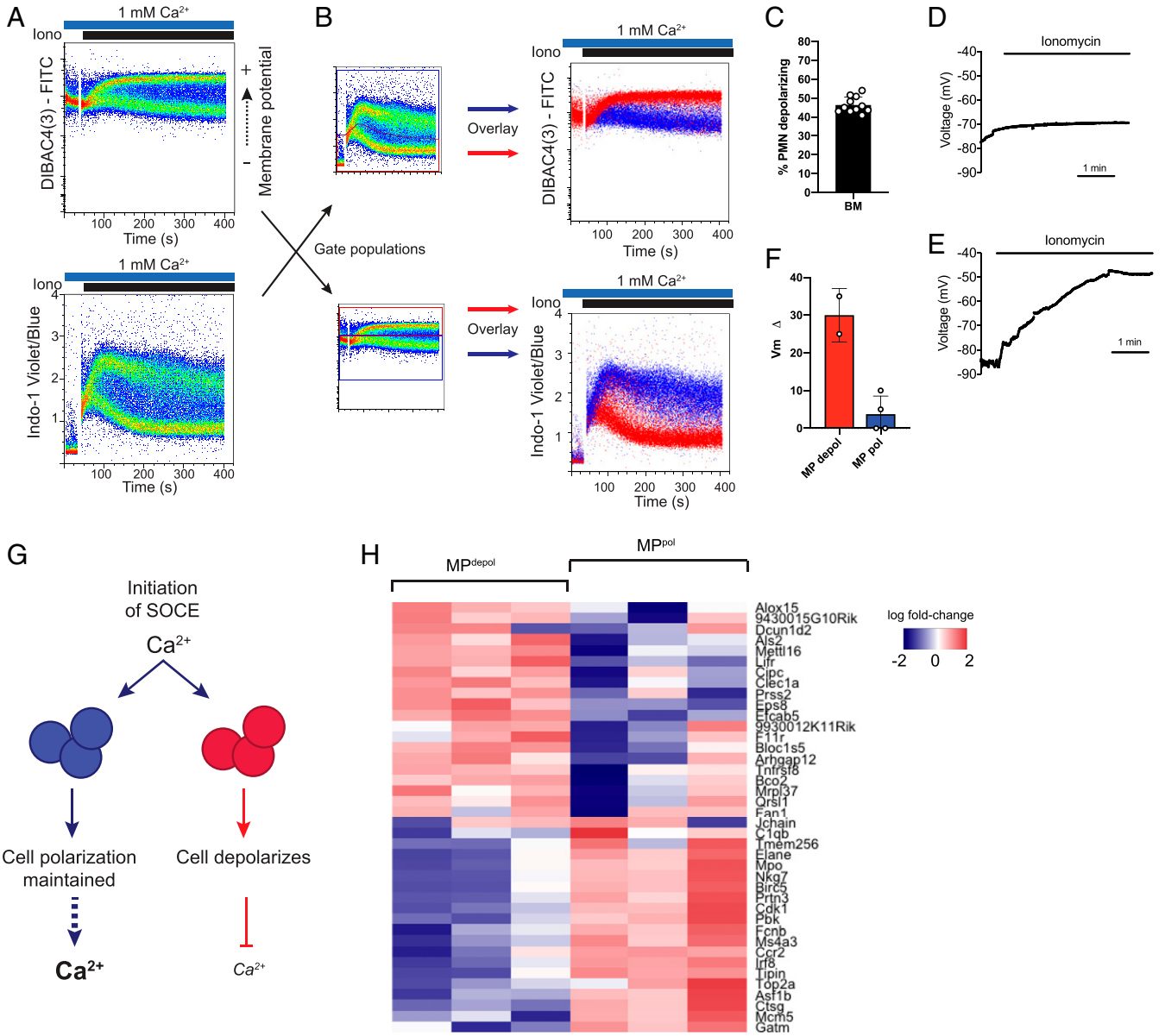

Fig. 4. Differential regulation of membrane potential in neutrophil subsets determines magnitude of SOCE. (*A*) Membrane potential (*Upper*) or calcium (*Lower*) was measured in isolated bone marrow neutrophils stimulated with ionomycin using the indicators DIBAC4(3) (membrane potential) and Indo-1 (calcium). (*B*) Bone marrow neutrophils were co-labeled with DIBAC4(3) and Indo-1 for simultaneous measurement of membrane potential and calcium flux by flow cytometry. Calcium subsets (gates shown; *B*, *Left*) were overlaid to show the relationship to membrane potential (*B*, *Upper*) or membrane potential subsets were overlaid to show the relationship to calcium (*B*, *Lower*). (*C*) Quantitation of percent of bone marrow (BM) neutrophils that typically depolarize, gates are shown in *SI Appendix*, Fig. S5*G*. $n = 11$ mice. (*D* and *E*) Current-clamp measurements of neutrophil membrane potential upon application of 100 nM ionomycin. Shown are representative tracings of cells that maintained polarization (*D*) or depolarized (*E*). (*F*) Quantitation of observed change in membrane potential (MP) from resting *Vm*. Total $n = 6$ cells. (*G*) Schematic demonstrating the proposed role of membrane potential in regulating calcium flux in these two neutrophil populations. Initiation of SOCE results in cell depolarization from influx of positive ions. In one subset, a compensatory mechanism/channel maintains cell polarization during SOCE, resulting in enhanced calcium influx. Conversely, a subset of cells depolarize, which decreases the driving force for calcium entry into the cell. (*H*) Heat map of RNAseq from sorted MP^{pol} vs. MP^{depol} subsets showing the top 20 up- and down-regulated genes. PMN, neutrophil.

fMLF receptor, FPR1 (fMLF), tyrosine kinase-associated Dectin-1 (Zymosan), and Fcγ-receptor (immobilized immune complexes), was significantly impaired in both single- and double-mutant neutrophils (Fig. 7 *A*–*C*). Neutrophils also synthesize LTB4 from arachidonic acid in a calcium-dependent manner (42, 43), and LTB4 release was decreased in all ORAI-deficient cells (Fig. 7*D*). Mobilization of secretory and secondary granules (CD18 and CD11b) was impaired only in *Orai1/2*^{VavCre} neutrophils; however, primary granule release (CD63), which requires a stronger stimulus, was impaired in both single and double ORAI mutant neutrophils (*SI Appendix*, Fig. S9 *A* and *B* and Fig. 7*E*). Similarly, phagocytosis was mildly impaired in ORAI1- and ORAI1/2-deficient, but not ORAI2-deficient, neutrophils (*SI Appendix*, Fig. S9*C*). These results support that ORAI1 and ORAI2 are required for multiple relevant aspects of calcium-dependent neutrophil function.

Loss of ORAI1 and ORAI2 Impairs Neutrophil-Mediated Host Defense against *S. aureus*. Since loss of ORAI1 and/or ORAI2 impaired neutrophil functions, we asked whether these deficiencies impaired neutrophil-mediated host defense. Host defense against

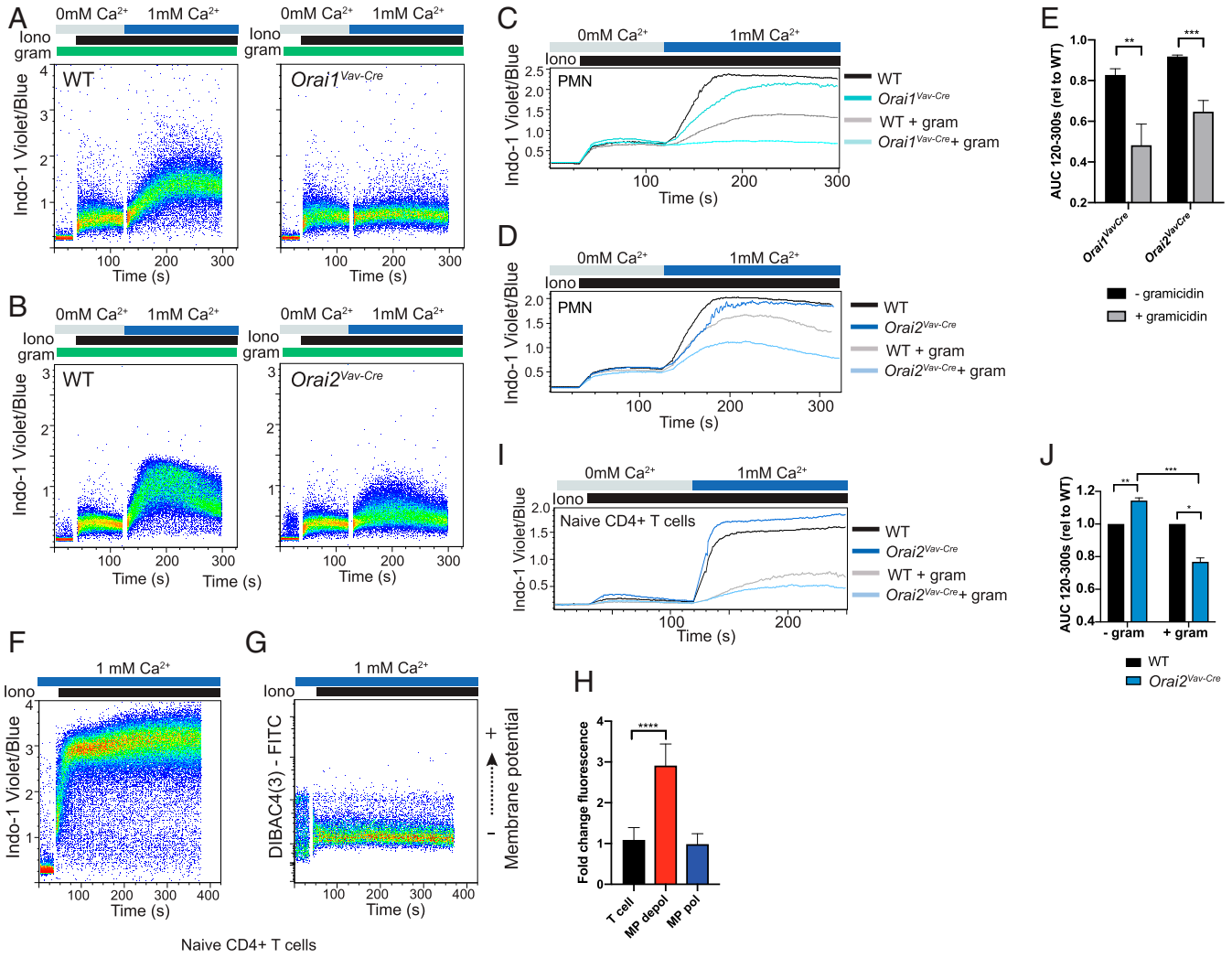

Fig. 5. Differential regulation of membrane potential confers distinct phenotype of Orai2 deficiency in neutrophils. (*A–G*) Calcium flux measured in WT, Orai1^{VavCre} (*A* and *C*), or Orai2^{VavCre} (*B* and *D*) neutrophils depolarized by pretreatment with the sodium ionophore gramicidin and stimulated with ionomycin. Dot plots are shown in *A* and *B*, and kinetic tracings of gramicidin (200 nM) treated vs. untreated cells are shown in *C* and *D*. (*E*) Quantification of data (*A–D*) from three to five independent experiments. (*F* and *G*) Calcium influx (*F*) or change in membrane potential (*G*) was measured by flow cytometry in WT isolated naïve CD4+ T cells showing a homogenous response. (*H*) Comparison of change in signal [DIBAC4(3) fluorescence] between naïve CD4+ T cells, and MP^{pol} or MP^{depol} neutrophils exposed to ionomycin. (*I* and *J*) Calcium influx measured in WT and Orai2^{VavCre} naïve CD4+ T cells either untreated or depolarized by pretreatment with the sodium ionophore gramicidin and stimulated with ionomycin 300 nM. Data shown are representative FACS plots or compiled data from two or three independent experiments, normalized to WT response. (*E*) Unpaired *t* test. (*H*) One-way ANOVA with Dunnett's test for multiple comparisons. (*J*) One-sample *t* test. *$P < 0.05$; **$P < 0.01$; ***$P < 0.001$; ****$P < 0.0001$. AUC, area under the curve; rel, relative. PMN, neutrophil.

S. aureus is known to require neutrophil ROS, as demonstrated by severe staphylococcal infections in patients with neutrophil defects, such as chronic granulomatous disease or congenital neutropenia. Indeed, *Orai1/2*^{VavCre} mice developed significantly larger lesions when challenged with *S. aureus* skin infection (Fig. 8 *A* and *B*). *Orai1*^{VavCre} mice also had larger lesions when compared with WT, although much smaller than ORAI1/2-deficient animals. No significant difference was seen in *Orai2*^{VavCre} mice. We saw no differences in bulk neutrophil recruitment to the lesions, as determined by Ly6G immunohistochemistry or myeloperoxidase enzyme-linked immunosorbent assay (ELISA) of lesion lysates; however, *Orai1/2*^{VavCre} mice had visible lakes of bacteria as observed via histology (Fig. 8 *C* and *D*) and higher bacterial burden at 72 h after infection (Fig. 8*E*). Of note, these experiments were performed in mice with total hematopoietic deletion of *Orai1* or *Orai2*, which limits our ability to conclude that these effects are primarily neutrophil-dependent. Unfortunately, genetic linkage between the neutrophil-specific *Mrp8–Cre* transgene and *Orai2* precluded use of this Cre in these experiments. However, we observed no difference in lesion size in *Orai1*^{VavCre} compared with *Orai1*^{Mrp8Cre} mice, and the time point postinfection is too early for an adaptive immune response to play a significant role, consistent with the conclusion that this phenotype is predominantly driven by neutrophil dysfunction (Fig. 8*F*).

Discussion

While SOCE is important for many aspects of neutrophil function, how the individual CRAC-channel components fine-tune calcium signaling remains unknown. Here, we demonstrate that ORAI1 and ORAI2 cooperatively regulate neutrophil SOCE and calcium-dependent responses, such that loss of both ORAI1 and ORAI2 renders mice susceptible to staphylococcal skin infection. Unlike other immune cells, loss of ORAI2 impairs SOCE in neutrophils. We show that the mechanism driving this unique phenotype

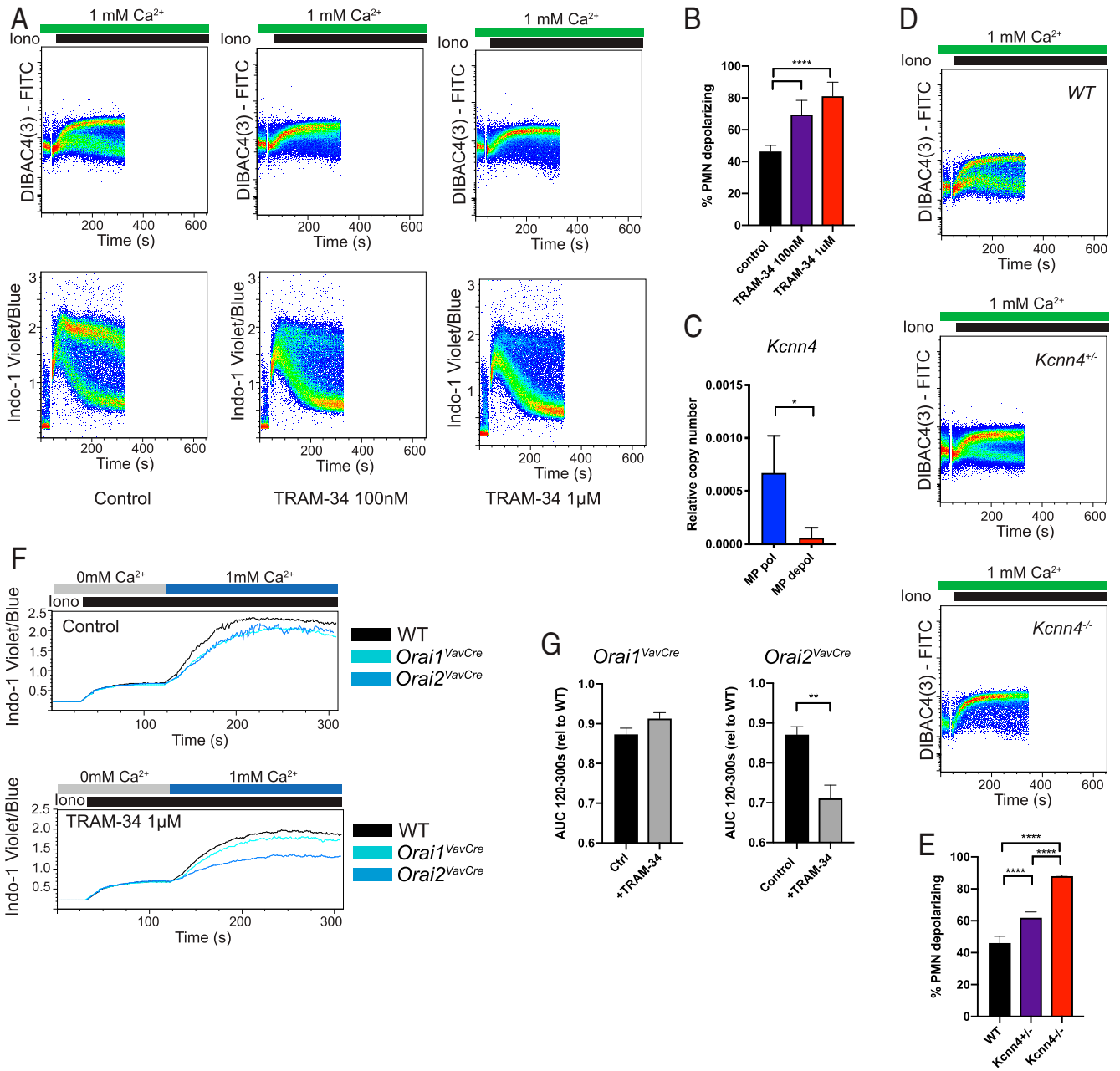

Fig. 6. Membrane potential in neutrophil subsets is determined by differential expression of KCa3.1/Kcnn4. (*A*) Membrane potential (*Upper*) or calcium (*Lower*) was measured in isolated bone marrow neutrophils stimulated with ionomycin (Iono). Cells were pretreated with vehicle (control) or TRAM-34 at the indicated concentration. (*B*) Quantification of percent neutrophils depolarizing from data in *A* compiled from three independent experiments. (*C*) qRT-PCR for expression of *Kcnn4* in neutrophils sorted from MP^{depol} and MP^{pol} populations during ionomycin stimulation. $n = 3$. (*D*) Membrane potential measured in isolated bone marrow neutrophils from WT, *Kcnn4*$^{+/-}$, or *Kcnn4*$^{-/-}$ mice, stimulated with ionomycin 100 nM. (*E*) Quantification of percent neutrophils in depolarized subset from data in *D* compiled from two to four independent experiments. (*F*) Calcium flux measured in WT, *Orai1*^{VavCre}, or *Orai2*^{VavCre} neutrophils pretreated with vehicle (*Upper*) or TRAM-34 at a concentration of 1 μM (*Lower*). (*G*) Quantitation of area under the curve (AUC) of *F*, combined from three independent experiments. (*B and E*) One-way ANOVA with Dunnett's test for multiple comparisons. (*F*) Unpaired *t* test. *$P < 0.05$; **$P < 0.01$; ***$P < 0.001$; ****$P < 0.0001$. Ctrl, control; rel, relative; PMN, neutrophil.

is, at least in part, related to regulation of membrane potential during SOCE, whereby depolarization of a subset of neutrophils correlates with impaired calcium influx in ORAI2-deficient cells. These findings show that ORAI1 and ORAI2 are the primary CRAC-channel components in mouse neutrophils, demonstrate important differences in function of ORAI family members among immune cells, and highlight the critical relationship between regulation of membrane potential and SOCE as a fundamental feature of neutrophil biology. Furthermore, these studies identify subpopulations of neutrophils with markedly different calcium signatures due to regulation of membrane potential by KCa3.1.

Our finding that ORAI2-deficient neutrophils display decreased SOCE is notable, given that Vaeth et al. (15) demonstrated, through a series of overexpression and electrophysiological experiments, that incorporation of ORAI2 into heteromeric channels dampens SOCE due to increased fast calcium-dependent inactivation. They concluded that SOCE is enhanced in ORAI2-deficient

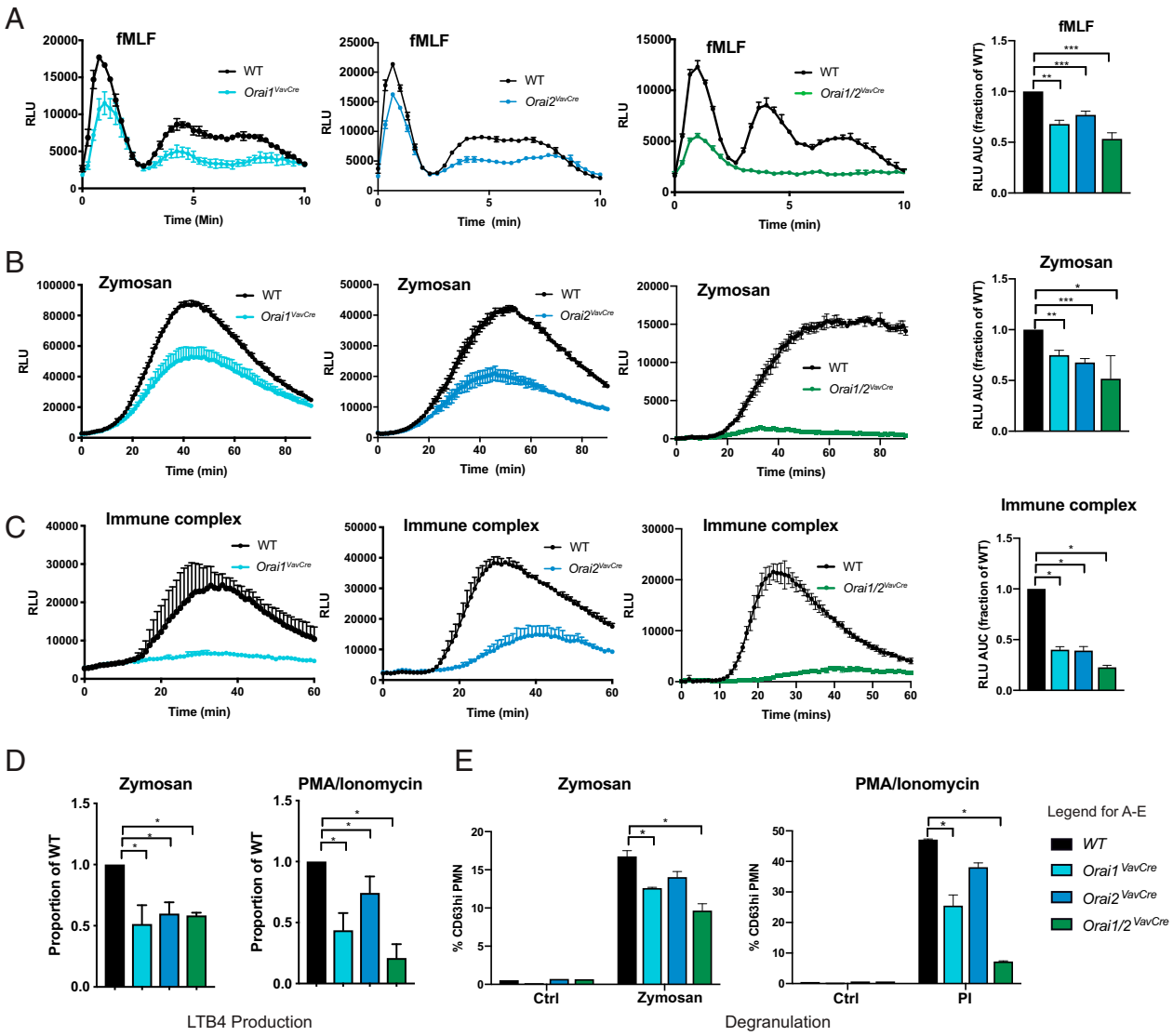

Fig. 7. Orai1 and Orai2 are required for neutrophil ROS, phagocytosis, and LTB4 production. (*A–C*) ROS production in WT, *Orai1*^{VavCre}, *Orai2*^{VavCre}, or *Orai1/2*^{VavCre} neutrophils stimulated by fMLF at a concentration of 10 μM (*A*), zymosan at a concentration of 20 μg/mL (*B*), or plate-bound immune complexes (*C*). (*A–C, Right*) Quantitation of AUC combined from three to eight independent experiments, normalized to WT response. One-sample *t* test. (*D* and *E*) Analysis of LTB4 production (*D*) and degranulation (*E*) by WT, *Orai1*^{VavCre}, *Orai2*^{VavCre}, or *Orai1/2*^{VavCre} neutrophils stimulated with zymosan (20 μg/mL) or PMA/Ionomycin (eBioscience cell stimulation mixture 1:4,000). Data in *D* are combined from five independent experiments, normalized to WT response, one-sample *t* test. Data in *E* are combined from three or four independent experiments, unpaired *t* test. *$P < 0.05$; **$P < 0.005$; ***$P < 0.0001$. RLU, relative luminescence units.

naïve CD4+ T cells, dendritic cells, and macrophages under such conditions (15). The ORAI2 targeting strategy used by Vaeth et al. (15) is different (knockout [KO] vs. Flox-Cre); however, we also found enhanced SOCE in naïve CD4+ T cells (Fig. 5 *I* and *J*), suggesting that differences in gene-targeting strategies are not contributory. In addition to the cell-type-specific differences in the *Orai2*$^{-/-}$ phenotype, we also observed that within mouse neutrophils, loss of ORAI2 preferentially impacts SOCE in the depolarized/Ca^{lo} subset. In contrast, loss of ORAI1 affects both polarized/Ca^{hi} and depolarized/Ca^{lo} populations. The simplest explanation for these observations is that ORAI1 and/or ORAI2 expression differs between the neutrophil populations; however, ORAI isoform expression levels were similar by qPCR and RNAseq. Furthermore, equalization of the subset membrane potentials in *Kcnn4*$^{-/-}$ neutrophils yields a homogeneous calcium (Ca^{lo}) response, suggesting that the enhanced calcium response of the polarized neutrophil subset is predominantly due to the state of the membrane potential, rather than differing levels of ORAI isoforms. We cannot exclude, however, that modulators of SOCE may differentially interact with ORAI2 vs. ORAI1 and also contribute to the observed phenotype.

An alternative hypothesis is that the membrane potential itself differentially influences the function of ORAI1- vs. ORAI2-containing channels. In support of this notion, inhibition of KCa3.1 in ORAI2-deficient cells switches the phenotype of polarized/Ca^{hi} cells to depolarized/Ca^{lo}. Under these conditions, the impact of ORAI2 deficiency is magnified. Furthermore, we demonstrated that ORAI2-deficient naïve CD4+ T cells phenocopy neutrophils under depolarized conditions, with the caveat that we cannot exclude nonspecific effects of gramicidin. These results support the notion that the cellular and/or subset phenotype of ORAI2 deficiency may be, at least in part, dependent on the regulation of the membrane potential during SOCE. ORAI channels are not voltage-gated; however, the membrane potential can influence features of CRAC-channel function, including the

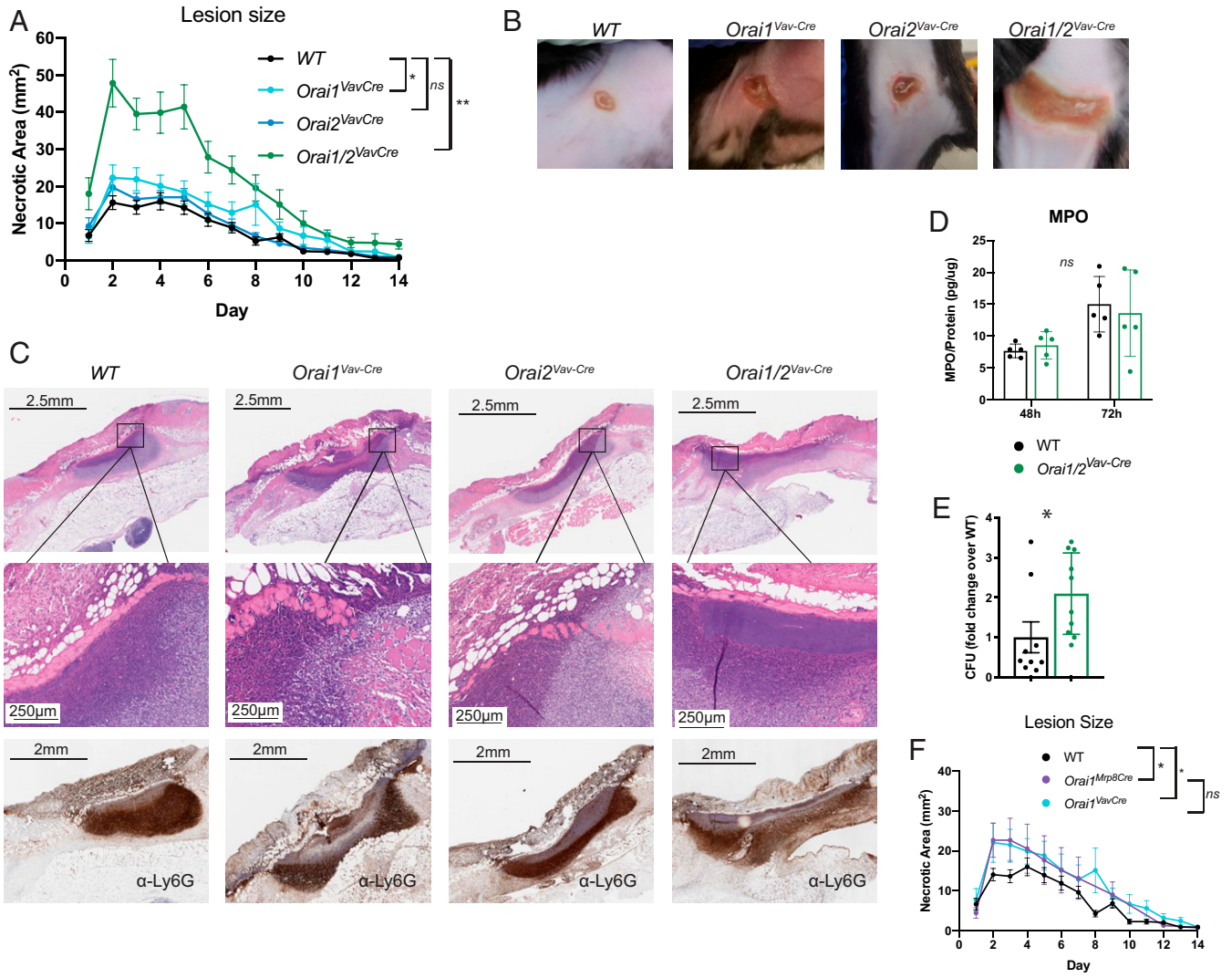

Fig. 8. Loss of Orai1 and Orai2 impairs host defense against *S. aureus*. (*A*) Skin infection with MRSA. WT, *Orai1*^{VavCre}, *Orai2*^{VavCre}, or *Orai1/2*^{VavCre} mice were infected intradermally with 10^8 CFU, and lesions were measured daily for 2 wk. Data represent lesion measurements from 10 to 25 mice, compiled from three to five independent experiments. (*B*) Representative photographs of lesions. (*C*, *Top* and *Middle*) Hematoxylin and eosin stains at low power (*Top*) and higher power (*Middle*). (*C*, *Bottom*) Immunohistochemistry with the neutrophil marker Ly6G. (*D*) Neutrophil infiltration into the lesion as determined by myeloperoxidase (MPO) ELISA of lesion lysates, normalized to lysate total protein. (*E*) CFU at 72 h from lesion lysates. (*F*) *WT*, *Orai1*^{VavCre}, and *Orai1*^{Mrp8Cre} mice were infected intradermally with 10^8 CFU, and lesions were measured daily for 2 wk. Data represent lesion measurements from 10 to 25 mice, compiled from two to five independent experiments. Note, since data represent mice compiled from multiple experiments, WT and *Orai1*^{VavCre} data are identical to data from *A*, shown here again for clarity. (*A* and *F*) Repeated-measures ANOVA. (*D* and *E*) Unpaired Student's *t* test. $*P < 0.05$; $**P < 0.005$. ns, not significant.

kinetics of channel opening and calcium-dependent potentiation, which could contribute to the observed phenotype (44). It must be noted that previous electrophysiological studies of *Orai2*$^{-/-}$ macrophages by Vaeth et al. (15) did not reveal this voltage dependence; however, these voltage–clamp experiments were performed under supraphysiological conditions to enhance the very small CRAC current (20 mM calcium); therefore, it is possible that the changes we saw were masked under those conditions. Further biochemical and electrophysiological studies, preferably in primary cells where the native ORAI/STIM/modulator ratios are preserved, will be necessary to clearly define the relationship of membrane potential and ORAI channel function.

Loss of ORAI2 also preferentially impairs SOCE at low concentrations of extracellular calcium. The free (ionized) calcium concentration in blood is tightly regulated between 1.05 and 1.3 mM. However, local calcium concentrations within an abscess, thrombus, or injured tissue vary due to changes in pH, oxygen tension, or enrichment in calcium-binding extracellular matrix proteins (45–47). Furthermore, hypocalcemia is common during sepsis and critical illness. Thus, the mechanics of SOCE under conditions of limiting extracellular calcium is highly relevant, particularly for neutrophils that are routinely found at such sites as the first line of defense.

We show here that the functional consequence of ORAI1 and/or ORAI2 deficiency in mice is reflected in multiple deficits, such as decreased activation of the NADPH oxidase, phagocytosis, and degranulation. There are subtle differences in the magnitude of defects between ORA1- and ORAI2-deficient cells (e.g., ORAI1 appeared to play a larger role in phagocytosis), which are not necessarily explained by absolute magnitude of SOCE. ORAI1 has been shown to associate with the phagosome (33), and further studies are required to determine the subcellular localization of ORAI1 vs. ORAI2 and association with signaling complexes involved in neutrophil responses. Of note, the magnitude of the

ROS defect (>50%) in ORAI1- or ORAI2-deficient cells appears out of proportion to the observed defect in SOCE (10 to 20%). Perhaps local concentrations of calcium around the NADPH oxidase are impacted more than whole-cell measures. Alternatively, our observation that depolarization magnifies the SOCE defect in ORAI-deficient cells suggests that inhibition of SOCE from ROS-mediated depolarization could initiate a negative-feedback mechanism that is exacerbated in ORAI mutant cells.

Neutrophil heterogeneity is an emerging area of neutrophil biology, and neutrophils with distinct functional characteristics have been described during infection, chronic inflammation, aging, and cancer (48–52). However, it has been difficult to distinguish whether these phenotypes represent predetermined neutrophil subtypes or a phenotype acquired in response to the microenvironment. Here, we identify transcriptionally distinct populations found in naïve mice, which feature typical neutrophil surface markers, but distinct calcium signatures due to differential expression of KCa3.1. Our results evoke numerous questions regarding the identity and function of neutrophils within these subsets. One hypothesis is that regulation of membrane potential is developmentally controlled and that these populations represent stages of neutrophil maturation, or senescent neutrophils upon return to the marrow from circulation. The transcriptional data showing increased expression of primary granule proteins and growth- and division-related genes in the MP^{pol} subset might support this notion of a developmental process, since primary granules are assembled in promyelocytes. Further analysis of immature as well as peripheral blood neutrophils will be necessary to answer this question. It is interesting to contemplate the functional significance of these discrete populations; since calcium influx is markedly enhanced in the MP^{pol} subset, one would anticipate that calcium-dependent neutrophil functions are enhanced in this population as well. The mechanisms controlling the development and function of these neutrophil subsets have implications for neutrophil function during infection, acute and chronic inflammation, and cancer and is an exciting avenue for further study.

Materials and Methods

Mice. *Orai1*$^{f/f}$ mice (Amgen) were described (53). *Orai2*$^{f/f}$ mice were generated by Taconic. The targeting vector was generated by using bacterial artificial chromosome (BAC) clones from the C57BL/6J RPCIB-731 BAC library and transfected into the TaconicArtemis C57BL/6N Tac embryonic stem cell line. LoxP sites were inserted by flanking intron 3 along with a polyadenylation signal (human growth hormone polyadenylation signal) inserted 3′ of the *Orai2* gene in order to prevent transcriptional read-through. Positive selection markers flanked by FRT (neomycin resistance) and F3 (Puromycin resistance) sites were inserted into intron 2 and downstream of the 3′ untranslated region, respectively. The conditional KO allele was obtained after in vivo Flp-mediated removal of the selection markers (*SI Appendix*, Fig. S1). Single- and double-mutant (*Orai1/2*$^{f/f}$) mice were bred to mice bearing transgenes with Cre recombinase under control of the *Vav* or human *S100A8* (*MRP8*) promoters (Jackson Labs). Mice were back-crossed more than eight generations on the C57BL6 background. Male and female mice were used. Controls were predominantly littermate (*flox/flox*) mice. Neutrophils from these mice functioned equivalently to *Vav–Cre* and *Mrp8–Cre* mice. Mice were maintained in an Association for Assessment and Accreditation of Laboratory Animal Care-accredited, specific pathogen-free barrier facilities at the University of California San Francisco or Washington University and used in accordance with approved institutional animal care and use committee protocols and the eighth edition of the *Guide for the Care and Use of Laboratory Animals* (54).

Neutrophil Isolation and Functional Studies. Bone marrow neutrophils were obtained as described by using a single-step Percoll gradient (55). Neutrophil respiratory burst was measured by a luminol-based chemiluminescent assay, as described (27). Immune complex-covered surfaces were prepared as described (56). Phagocytosis was assayed as described (19). To assay degranulation, isolated neutrophils (2×10^5) were stimulated in 96-well plates for 45 min with the indicated agonist. Cells were stained for surface markers of degranulation (CD11b, CD18, and CD63) and analyzed by flow cytometry. Additional details are found in *SI Appendix*.

Measurement of Intracellular Calcium Levels. Calcium measurements by flow cytometry were described (19). Additional details are found in *SI Appendix*.

Measurement of Membrane Potential by Flow Cytometry. To measure membrane potential, cells were incubated with the membrane-potential-sensitive dye, DiBAC4(3) (250 nM) for 10 min, and then change in fluorescence (FITC channel) was measured during stimulation via flow cytometry. In some experiments, DiSBAC2(3) (250 nM) or oxonol VI (2 μM) were used, and fluorescence was measured in the phycoerythrin or allophycocyanin channels, respectively. To allow comparison of relative changes in membrane potential across experiments, data are expressed as fold change in fluorescence over baseline. For calibration, neutrophils were resuspended in buffer with 5, 10, 20, 30, 60, or 90 mM KCl in the presence of 2 μM valinomycin. The approximate *Vm* was calculated by using the Nernst equation.

Electrophysiology. Patch-clamp recordings were performed by using an Axopatch 200B amplifier paired to a Digidata 1550 digitizer with pClamp 10.4 software. For measuring changes in mouse neutrophil membrane potential, we used the perforated patch configuration of the patch-clamp technique in current-clamp mode. The patch electrodes were prepared from borosilicate glass capillaries (WPI) and had a resistance of 5.0 to 6.0 MΩ when filled with pipette solution. Freshly isolated cells were perfused with Krebs–Ringer buffer of the following composition (in mM): 129 NaCl, 5 $NaHCO_3$, 4.8 KCl, 1.2 KH_2PO_4, 2.5 $CaCl_2$, 2.4 $MgSO_4$, 1 glucose, 10 HEPES (pH 7.4, adjusted with NaOH); osmolarity was adjusted to 300 mOsm/kg with mannitol. The pipettes were filled with solution (in mM): 140 KCl, 1 $MgCl_2$, 10 ethylene glycol-*bis*(β-aminoethyl ether)-*N*,*N*,*N*′,*N*′-tetraacetic acid and 10 Hepes (pH 7.25, adjusted with KOH), and 295 mOsm/kg, and contained 240 μg/mL amphotericin B (Sigma-Aldrich, catalog no. A9528). All experiments were carried out at 32 to 33 °C.

***S. aureus* Skin Infection.** Mice were anesthetized; their flanks were depilated by using Nair, and 3×10^7 methicillin-resistant *S. aureus* (USA300 strain) was injected intradermally (57). Lesions (abscess and necrotic area) were measured daily over the course of 14 d. For a subset, mice were killed at the indicated time points, and lesions were excised for histology or homogenized to determine bacterial colony-forming units (CFUs) and neutrophil infiltration by myeloperoxidase ELISA (RD Systems). Histology (hematoxylin and eosin [H&E] and Ly6G IHC) was performed by HistoWiz.

Additional detailed methods can be found in *SI Appendix*.

Data Availability. RNAseq data are available in the Gene Expression Omnibus database, accession number GSE157200 (37). Unique reagents (including Orai2-flox mice) are available upon request from the corresponding author (R.C.).

ACKNOWLEDGMENTS. We thank Mary Dinauer and Bob Mecham for critical reading of the manuscript. This work was supported by NIH Grants AI65495 and AI68150 (to C.A.L.) and K08AI119134 (to R.A.C.); and the Children's Discovery Institute of Washington University and St. Louis Children's Hospital (R.A.C.). R.A.C. was a Fellow of the Pediatric Scientist Development Program, supported by Eunice Kennedy Shriver National Institute of Child Health and Human Development Grant K12-HD000850.

1. R. A. Clemens, C. A. Lowell, CRAC channel regulation of innate immune cells in health and disease. *Cell Calcium* **78**, 56–65 (2019).
2. A. Lis *et al*., CRACM1, CRACM2, and CRACM3 are store-operated Ca2+ channels with distinct functional properties. *Curr. Biol.* **17**, 794–800 (2007).
3. W. I. DeHaven, J. T. Smyth, R. R. Boyles, J. W. Putney Jr., Calcium inhibition and calcium potentiation of Orai1, Orai2, and Orai3 calcium release-activated calcium channels. *J. Biol. Chem.* **282**, 17548–17556 (2007).
4. M. Fukushima, T. Tomita, A. Janoshazi, J. W. Putney, Alternative translation initiation gives rise to two isoforms of Orai1 with distinct plasma membrane mobilities. *J. Cell Sci.* **125**, 4354–4361 (2012).
5. S. A. Gross *et al*., Murine ORAI2 splice variants form functional Ca2+ release-activated Ca2+ (CRAC) channels. *J. Biol. Chem.* **282**, 19375–19384 (2007).
6. T. Kawasaki, T. Ueyama, I. Lange, S. Feske, N. Saito, Protein kinase C-induced phosphorylation of Orai1 regulates the intracellular Ca2+ level via the store-operated Ca2+ channel. *J. Biol. Chem.* **285**, 25720–25730 (2010).
7. S. Saul *et al*., A calcium-redox feedback loop controls human monocyte immune responses: The role of ORAI Ca2+ channels. *Sci. Signal.* **9**, ra26 (2016).
8. B. A. Niemeyer, Changing calcium: CRAC channel (STIM and Orai) expression, splicing, and posttranslational modifiers. *Am. J. Physiol. Cell Physiol.* **310**, C701–C709 (2016).

9. R. Palty, A. Raveh, I. Kaminsky, R. Meller, E. Reuveny, SARAF inactivates the store operated calcium entry machinery to prevent excess calcium refilling. *Cell* **149**, 425–438 (2012).
10. S. Srikanth *et al*., Junctate is a Ca2+-sensing structural component of Orai1 and stromal interaction molecule 1 (STIM1). *Proc. Natl. Acad. Sci. U.S.A.* **109**, 8682–8687 (2012).
11. S. Feske *et al*., A mutation in Orai1 causes immune deficiency by abrogating CRAC channel function. *Nature* **441**, 179–185 (2006).
12. M. Prakriya *et al*., Orai1 is an essential pore subunit of the CRAC channel. *Nature* **443**, 230–233 (2006).
13. Y. Gwack *et al*., Hair loss and defective T- and B-cell function in mice lacking ORAI1. *Mol. Cell. Biol.* **28**, 5209–5222 (2008).
14. M. Vig *et al*., Defective mast cell effector functions in mice lacking the CRACM1 pore subunit of store-operated calcium release-activated calcium channels. *Nat. Immunol.* **9**, 89–96 (2008).
15. M. Vaeth *et al*., ORAI2 modulates store-operated calcium entry and T cell-mediated immunity. *Nat. Commun.* **8**, 14714 (2017).
16. L. Bei, T. Hu, Z. M. Qian, X. Shen, Extracellular Ca2+ regulates the respiratory burst of human neutrophils. *Biochim. Biophys. Acta* **1404**, 475–483 (1998).
17. M. M. Boucek, R. Snyderman, Calcium influx requirement for human neutrophil chemotaxis: Inhibition by lanthanum chloride. *Science* **193**, 905–907 (1976).
18. S. Bréchard, S. Plançon, C. Melchior, E. J. Tschirhart, STIM1 but not STIM2 is an essential regulator of Ca2+ influx-mediated NADPH oxidase activity in neutrophil-like HL-60 cells. *Biochem. Pharmacol.* **78**, 504–513 (2009).
19. R. A. Clemens, J. Chong, D. Grimes, Y. Hu, C. A. Lowell, STIM1 and STIM2 cooperatively regulate mouse neutrophil store-operated calcium entry and cytokine production. *Blood* **130**, 1565–1577 (2017).
20. N. Demaurex, S. Saul, The role of STIM proteins in neutrophil functions. *J. Physiol.* **596**, 2699–2708 (2018).
21. R. Immler, S. I. Simon, M. Sperandio, Calcium signalling and related ion channels in neutrophil recruitment and function. *Eur. J. Clin. Invest.* **48** (suppl. 2), e12964 (2018).
22. K. Itagaki *et al*., Store-operated calcium entry in human neutrophils reflects multiple contributions from independently regulated pathways. *J. Immunol.* **168**, 4063–4069 (2002).
23. C. Lee *et al*., Store-operated calcium channel inhibition attenuates neutrophil function and postshock acute lung injury. *J. Trauma* **59**, 56–63, discussion 63 (2005).
24. U. Y. Schaff *et al*., Orai1 regulates intracellular calcium, arrest, and shape polarization during neutrophil recruitment in shear flow. *Blood* **115**, 657–666 (2010).
25. N. Steinckwich *et al*., Potent inhibition of store-operated Ca2+ influx and superoxide production in HL60 cells and polymorphonuclear neutrophils by the pyrazole derivative BTP2. *J. Leukoc. Biol.* **81**, 1054–1064 (2007).
26. N. Steinckwich *et al*., Role of the store-operated calcium entry protein, STIM1, in neutrophil chemotaxis and infiltration into a murine model of psoriasis-inflamed skin. *FASEB J.* **29**, 3003–3013 (2015).
27. H. Zhang *et al*., STIM1 calcium sensor is required for activation of the phagocyte oxidase during inflammation and host defense. *Blood* **123**, 2238–2249 (2014).
28. S. Bréchard, C. Melchior, S. Plançon, V. Schenten, E. J. Tschirhart, Store-operated Ca2+ channels formed by TRPC1, TRPC6 and Orai1 and non-store-operated channels formed by TRPC3 are involved in the regulation of NADPH oxidase in HL-60 granulocytes. *Cell Calcium* **44**, 492–506 (2008).
29. N. Steinckwich, V. Schenten, C. Melchior, S. Bréchard, E. J. Tschirhart, An essential role of STIM1, Orai1, and S100A8-A9 proteins for Ca2+ signaling and FcγR-mediated phagosomal oxidative activity. *J. Immunol.* **186**, 2182–2191 (2011).
30. N. Dixit *et al*., Leukocyte function antigen-1, kindlin-3, and calcium flux orchestrate neutrophil recruitment during inflammation. *J. Immunol.* **189**, 5954–5964 (2012).
31. R. Elling *et al*., Preserved effector functions of human ORAI1- and STIM1-deficient neutrophils. *J. Allergy Clin. Immunol.* **137**, 1587–1591.e7 (2016).
32. G. Sogkas *et al*., Orai1 controls C5a-induced neutrophil recruitment in inflammation. *Eur. J. Immunol.* **45**, 2143–2153 (2015).
33. P. Nunes *et al*., STIM1 juxtaposes ER to phagosomes, generating Ca^{2+} hotspots that boost phagocytosis. *Curr. Biol.* **22**, 1990–1997 (2012).
34. X. Cai *et al*., The Orai1 store-operated calcium channel functions as a hexamer. *J. Biol. Chem.* **291**, 25764–25775 (2016).
35. V. Tsvilovskyy *et al*., Deletion of Orai2 augments endogenous CRAC currents and degranulation in mast cells leading to enhanced anaphylaxis. *Cell Calcium* **71**, 24–33 (2018).
36. P. G. Hogan, A. Rao, Store-operated calcium entry: Mechanisms and modulation. *Biochem. Biophys. Res. Commun.* **460**, 40–49 (2015).
37. D. Grimes, *et al*, Differential regulation of membrane potential during store-operated calcium entry in neutrophil subsets. GEO database. https://www.ncbi.nlm.nih.gov/geo/query/acc.cgi?acc=GSE157200. Deposited 30 August 2020.
38. D. Morgan *et al*., Sustained activation of proton channels and NADPH oxidase in human eosinophils and murine granulocytes requires PKC but not cPLA2 alpha activity. *J. Physiol.* **579**, 327–344 (2007).
39. R. Murphy, T. E. DeCoursey, Charge compensation during the phagocyte respiratory burst. *Biochim. Biophys. Acta* **1757**, 996–1011 (2006).
40. E. Y. Chiang *et al*., Potassium channels Kv1.3 and KCa3.1 cooperatively and compensatorily regulate antigen-specific memory T cell functions. *Nat. Commun.* **8**, 14644 (2017).
41. C. M. Fanger *et al*., Calcium-activated potassium channels sustain calcium signaling in T lymphocytes. Selective blockers and manipulated channel expression levels. *J. Biol. Chem.* **276**, 12249–12256 (2001).
42. O. Rådmark, O. Werz, D. Steinhilber, B. Samuelsson, 5-Lipoxygenase, a key enzyme for leukotriene biosynthesis in health and disease. *Biochim. Biophys. Acta* **1851**, 331–339 (2015).
43. C. C. Leslie, Cytosolic phospholipase A_2: Physiological function and role in disease. *J. Lipid Res.* **56**, 1386–1402 (2015).
44. A. Zweifach, R. S. Lewis, Calcium-dependent potentiation of store-operated calcium channels in T lymphocytes. *J. Gen. Physiol.* **107**, 597–610 (1996).
45. P. Maurer, E. Hohenester, J. Engel, Extracellular calcium-binding proteins. *Curr. Opin. Cell Biol.* **8**, 609–617 (1996).
46. E. M. Brown, P. M. Vassilev, S. C. Hebert, Calcium ions as extracellular messengers. *Cell* **83**, 679–682 (1995).
47. W. G. Owen, J. Bichler, D. Ericson, W. Wysokinski, Gating of thrombin in platelet aggregates by pO2-linked lowering of extracellular Ca2+ concentration. *Biochemistry* **34**, 9277–9281 (1995).
48. B. Uhl *et al*., Aged neutrophils contribute to the first line of defense in the acute inflammatory response. *Blood* **128**, 2327–2337 (2016).
49. C. Silvestre-Roig, A. Hidalgo, O. Soehnlein, Neutrophil heterogeneity: Implications for homeostasis and pathogenesis. *Blood* **127**, 2173–2181 (2016).
50. J. Y. Sagiv *et al*., Phenotypic diversity and plasticity in circulating neutrophil subpopulations in cancer. *Cell Rep.* **10**, 562–573 (2015).
51. O. Marini *et al*., Mature $CD10^+$ and immature $CD10^-$ neutrophils present in G-CSF-treated donors display opposite effects on T cells. *Blood* **129**, 1343–1356 (2017).
52. J. Pillay *et al*., Functional heterogeneity and differential priming of circulating neutrophils in human experimental endotoxemia. *J. Leukoc. Biol.* **88**, 211–220 (2010).
53. A. Somasundaram *et al*., Store-operated CRAC channels regulate gene expression and proliferation in neural progenitor cells. *J. Neurosci.* **34**, 9107–9123 (2014).
54. National Research Council, *Guide for the Care and Use of Laboratory Animals* (National Academies Press, Washington, DC, ed. 8, 2011).
55. A. Mócsai, M. Zhou, F. Meng, V. L. Tybulewicz, C. A. Lowell, Syk is required for integrin signaling in neutrophils. *Immunity* **16**, 547–558 (2002).
56. T. Németh, K. Futosi, C. Sitaru, J. Ruland, A. Mócsai, Neutrophil-specific deletion of the CARD9 gene expression regulator suppresses autoantibody-induced inflammation in vivo. *Nat. Commun.* **7**, 11004 (2016).
57. R. E. Becker, B. J. Berube, G. R. Sampedro, A. C. DeDent, J. Bubeck Wardenburg, Tissue-specific patterning of host innate immune responses by Staphylococcus aureus α-toxin. *J. Innate Immun.* **6**, 619–631 (2014).